



HAL
open science

Interest of molecular/crystalline dispersions for the determination of solubility curves of drugs into polymers

M. Latreche, Jean-François Willart, M. Guerain, F. Danède, Alain Hédoux

► To cite this version:

M. Latreche, Jean-François Willart, M. Guerain, F. Danède, Alain Hédoux. Interest of molecular/crystalline dispersions for the determination of solubility curves of drugs into polymers. International Journal of Pharmaceutics, 2019, 570, pp.118626. 10.1016/j.ijpharm.2019.118626 . hal-02363477

HAL Id: hal-02363477

<https://hal.science/hal-02363477>

Submitted on 20 Oct 2020

HAL is a multi-disciplinary open access archive for the deposit and dissemination of scientific research documents, whether they are published or not. The documents may come from teaching and research institutions in France or abroad, or from public or private research centers.

L'archive ouverte pluridisciplinaire **HAL**, est destinée au dépôt et à la diffusion de documents scientifiques de niveau recherche, publiés ou non, émanant des établissements d'enseignement et de recherche français ou étrangers, des laboratoires publics ou privés.

INTEREST OF MOLECULAR / CRYSTALLINE DISPERSIONS FOR THE DETERMINATION OF SOLUBILITY CURVES OF DRUGS INTO POLYMERS

M. Latreche, J.F. Willart, M. Guerain, F Danède, A. Hédoux

Univ. Lille, CNRS, INRA, ENSCL, UMR 8207

UMET - Unité Matériaux et Transformations

F-59000 Lille, France

Corresponding author: jean-francois.willart@univ-lille1.fr

Abstract

We present here a method to increase the dissolution rate of drugs into polymers in order to make easier and faster the determination of the solubility curves of these mixtures. The idea is to prepare molecular/crystalline dispersions (MCD) where the drug is dispersed into the polymer, partly at the molecular level and partly in the form of small crystallites. We show that this particular microstructure greatly increases the dissolution rate of crystallites since: (1) The molecular dispersion has a plasticizing effect which greatly increases the molecular mobility in the amorphous matrix. (2) The fine crystallite dispersion in the matrix strongly reduces the distances over which the drug molecules have to diffuse to invade homogeneously the polymer by dissolution. MCD are here obtained by combining solid-state co-amorphization by high energy mechanical milling and then recrystallization by annealing under a plasticizing atmosphere. We have used MCD to determine the solubility lines of the two polymorphic forms (I and II) of sulindac into PVP. The investigations have been performed mainly by DSC and powder x-ray diffraction.

1. INTRODUCTION

Solubility¹⁻³ and physical stability⁴⁻⁸ are two essential properties of a drug. A good solubility is required to get a good bioavailability of the drug and a good physical stability is required to get a reasonable shelf life time. Of course, the most stable physical form of a drug is the crystalline form because it has the lowest free enthalpy¹. However, the crystalline form is also generally the less soluble. The best solubility is on the contrary provided by the amorphous form which is in a much higher free enthalpy level^{9,10}. However, amorphous materials are intrinsically unstable, and return unavoidably toward their crystalline state more or less rapidly and lose their improved solubility. It thus appears clearly that solubility and physical stability are antagonist properties which seem difficult to reconcile. And this problem is all the more crucial that the new drug molecules are more and more complex and thus less and less soluble³. There is thus an increasing necessity to formulate drugs in the amorphous state in order to increase their solubility. And this requires to find formulation protocols which are able to stabilize this amorphous state¹¹⁻¹⁴.

A possible way to stabilize a drug in an amorphous state is to make a molecular dispersion of this drug into an amorphous polymer^{12,15-18}. In such a system, the amorphous character of the drug is guaranty as long as the concentration of the drug into the polymer remains below the solubility limit of the drug into the polymer. It is thus essential to determine the solubility line of the mixture to optimize the formulation and to define the maximum drug that can be loaded into the polymer without a risk of recrystallization. However, this line is very difficult to determine¹⁹⁻²². The difficulty mainly comes from the very high viscosity of polymers which slows the dissolution processes and makes the equilibrium saturated state very difficult to

1 reach in practice. That's why the determination of solubility curve is so difficult and
2 very time consuming.

3 In this paper, we show how to enhance the dissolution rate of drugs into
4 polymers and how to take advantage of this faster dissolution to determine more
5 easily their solubility lines. The enhancement of the dissolution rate is obtained by
6 designing a specific microstructure of the initial physical mixture. This microstructure
7 is obtained through a protocol which combines milling stage and annealing stage
8 under plasticizing atmosphere.

9 The above protocol, and its effect on the dissolution rate, will be illustrated in
10 the case of the dissolution of sulindac ($C_{20}H_{17}FO_3S$) into PVP (polyvinylpyrrolidone).
11 Sulindac is a nonsteroidal anti-inflammatory agent which can form three crystalline
12 polymorphs: Forms I which crystallizes in the space group $P2_1/c$ ²³, form II which
13 crystallizes in the space group $Pbca$ ²⁴ and form IV which crystallizes in the space
14 group $P2_1/c$ ²⁵. Moreover, we will take advantage of the higher dissolution rate to
15 determine the solubility line of both form I and form II of sulindac into PVP.

16

17

18

1 2. EXPERIMENTALS

2 **Crystalline sulindac** (C₂₀ H₁₇ F O₃ S) was provided by SIGMA[®] life science
3 and used without any further purification.

4 **Amorphous PVP K12 PF** (M_w = 2000-3000 g.mol⁻¹, 5% w/w moisture) was
5 kindly provided by BASF and was used without purification

6 **Milling and co-milling** were performed in a high energy planetary mill
7 (pulverisette 7 – Fritsch). We used ZrO₂ milling jar of 45 cm³ with seven balls (Ø =
8 1cm) of the same material. 1 g of material was placed in the planetary mill
9 corresponding to a ball/sample weight ratio of 75:1. The rotation speed of the solar
10 disk was set to 400 rpm. All the milling and co-milling operations have been
11 performed during 10 hours in at room temperature. We took care to alternate milling
12 periods (typically 10 min) with pause periods (typically 5 min) in order to limit the
13 mechanical heating of the sample.

14 **Annealing under ethanol atmosphere** were performed at room temperature
15 (RT) by placing samples into a desiccator containing liquid ethanol.

16 **Differential Scanning Calorimetry (DSC)** and temperature modulated DSC
17 (MDSC) experiments were performed with the DSC Discovery of TA Instruments. For
18 all experiments, the sample was placed in an open aluminum pan (container with no
19 cover) and was flushed with highly pure nitrogen gas. Temperature and enthalpy
20 readings were calibrated using pure indium at the same scan rates and with the
21 same kind of pans used in the experiments. All DSC scans were performed at the
22 rate of 5°C/min. All MDSC scans were performed at 5°C/min using a modulation
23 amplitude of 0.663°C and a modulation period of 50 sec.

1 **Powder X-ray diffraction (PXRD)** experiments were performed with a
2 PanAlytical X'PERT PRO MPD diffractometer ($\lambda_{\text{CuK}\alpha} = 1.5418 \text{ \AA}$ for combined $\text{K}\alpha_1$
3 and $\text{K}\alpha_2$) equipped with an X'celerator detector (Almlo, The Netherlands). Samples
4 were placed into Lindemann glass capillaries ($\varnothing = 0.7\text{mm}$) and installed on a rotating
5 sample holder to avoid any artifacts due to preferential orientations of crystallites.
6 Thermal treatments, when needed, were performed in the calorimeter furnace using
7 the same conditions and parameters than those used for the DSC scans. Samples
8 were then rapidly cooled to RT, removed from the DSC pan and analyzed by PXRD.
9 This procedure guaranties a very accurate control of the sample temperature and a
10 perfect coherence between DSC and PXRD analysis.

11

1 3. POTENTIAL INFLUENCE OF THE MICROSTRUCTURE

2 ON THE DISSOLUTION RATE OF DRUGS INTO POLYMERS

3 Several methods have already been proposed to determine the solubility of a
4 drug into a polymer at a temperature T_a ¹⁹, but most of them require to reach the
5 equilibrium saturated state of the drug/polymer system at this temperature^{20-22,26-29}.
6 This state is generally obtained by annealing a mixture of the crystalline drug and the
7 polymer at T_a . The annealing time required to reach the equilibrium saturation is
8 generally very long because of the low molecular mobility in the polymer. Moreover,
9 the mobility in the polymer matrix decreases upon cooling, so that reaching the
10 equilibrium saturation in a reasonable time becomes rapidly impossible when T_a
11 approaches the glass transition temperature (T_g) of the polymer. This makes these
12 investigations tedious and very time consuming. However, it can be foreseen that the
13 microstructure of the mixture can also have a strong repercussion on the dissolution
14 rate.

15 This point is illustrated in figure 1 which shows two different microstructures.
16 The microstructure (a) simply corresponds to a physical mixture (PM) of drug and
17 polymer. The microstructure (b) is more sophisticated as the drug is dispersed into
18 the polymer, both at the molecular level and in the form of a myriad of crystallites,
19 giving rise to what is called: a molecular/crystalline dispersion (MCD). It can be easily
20 foreseen that the dissolution of the drug into the polymer will be faster in the MCD
21 than in the PM. This is due, in particular, to the fine dispersion of the crystallites
22 inside the polymer matrix that increases both the interface drug/polymer and the
23 number of diffusion centers of the drug. This also shortens strongly the average

1 diffusion length required for the drug molecules to invade homogeneously a polymer
2 grain. Moreover, the plasticizing effect of the molecular dispersion is expected to also
3 increase the dissolution rate by increasing the molecular mobility in the polymer
4 matrix.

5 In the following sections we will show: (i) how to produce molecular/crystalline
6 dispersions (MCD), (ii) to what extent the dissolution is faster in MCD than in physical
7 mixtures, (iii) how to take advantage of this faster dissolution to determine solubility
8 curves. All the investigations will be performed with the PVP / sulindac binary system.

9

10 **4. PROTOCOL TO OBTAIN MOLECULAR/CRYSTALLINE DISPERSIONS (MCD)**

11 Molecular/crystalline dispersions (MCD) of sulindac into PVP can be obtained
12 in two stages as illustrated in the bottom part of figure 1. In the first stage, a
13 supersaturated glass solution PVP/sulindac is produced, directly in the solid state, by
14 high energy milling of a physical mixture of the two components³⁰⁻³³. In the second
15 stage, the supersaturated glass solution is annealed in a plasticizing solvent
16 atmosphere. This increases the molecular mobility in the glass solution and makes it
17 possible the recrystallization of the excess drug dissolved in the polymer matrix. After
18 drying to remove the traces of solvent, the partially recrystallized sample appears to
19 be a MCD. The crystallites of drug are then randomly dispersed inside the glass
20 solution which has a lower drug concentration. The next two sections show the
21 experimental details which prove the feasibility of this protocol.

22

1 **4.1 Formation of glass solutions by co-milling and co-melting**

2 The objective of this section is to demonstrate the possibility to obtain glass
3 solutions PVP/sulindac by mechanical milling. Figure 2 shows the X-ray diffraction
4 patterns of pure sulindac, pure PVP and a physical mixture [15:85] of PVP and
5 sulindac, recorded before and after a 10 hour milling process. Before milling, the X-
6 ray diffraction pattern of sulindac shows many well defined Bragg peaks
7 characteristic of the crystalline form II²⁴. After milling, these Bragg peaks have totally
8 disappeared so that the material appears to be X-ray amorphous. This indicates that
9 milling has induced a total amorphization of sulindac (within the detection limit of
10 crystallites by PXRD). The X-ray diffraction patterns of PVP recorded before and
11 after milling are identical and free of any Bragg peaks. This indicates that PVP is
12 amorphous and does not undergo structural changes upon milling. The X-ray
13 diffraction pattern of the physical mixture shows the Bragg peak of sulindac form II.
14 After milling, the mixture is X-ray amorphous indicating the amorphization of the
15 crystalline fraction of sulindac (within the detection limit of crystallites by PXRD).
16 However, at this stage, it is not possible to decide if the co-milling has given rise to a
17 physical mixture of amorphous sulindac and amorphous PVP, or to a homogeneous
18 glass solution of the two components.

19 Figure 3 shows the heating (5°C/min) DSC scans of the previous samples.
20 Runs 1 and 2 correspond to pure sulindac before and after a 10 hour milling process.
21 Before milling (run 1), the thermogram only shows one endotherm corresponding to
22 the melting of form II. The melting temperature ($T_m = 186^\circ\text{C}$) and the melting enthalpy
23 ($\Delta H_m = 85 \text{ J/g}$) are consistent with the values reported in the literature³⁴. After milling
24 (run 2), the thermogram shows a C_p jump ($\Delta C_p = 0.40 \text{ J/g}^\circ\text{C}$) characteristic of a

1 glass transition at $T_g = 75^\circ\text{C}$ followed by a recrystallization exotherm ranging from 95
2 to 110°C . The recrystallization confirms the amorphization which has occurred during
3 milling and the glass transition indicates that the amorphous sample thus obtained
4 has a glassy character. Such a solid state amorphization upon milling was recently
5 reported³⁵ and it was noted that the recrystallization upon heating of the sample
6 amorphized by milling occurs toward form I. Runs 4 and 5 correspond to pure PVP
7 before and after milling. The two thermograms are identical and only show a glass
8 transition at $T_g = 110^\circ\text{C}$ ($\Delta C_p = 0.35 \text{ J/g}^\circ\text{C}$). The fact that T_g is not affected by the
9 milling process indicates that the polymer chains were not severely broken during the
10 milling process. Run 3 corresponds to the physical mixture milled 10 hours. It shows
11 a strong recrystallization ranging from 115°C to 140°C that confirms the complete
12 amorphization of sulindac during milling. A C_p jump is also clearly detected at $T_g =$
13 78°C i.e. a few degrees above the glass transition of pure sulindac. Such a single
14 glass transition occurring between those of the pure compounds indicates that the
15 co-milling has given rise to a homogeneous glass solution and not to a mere physical
16 mixture of amorphous sulindac and amorphous PVP. Moreover, the strong
17 recrystallization occurring at higher temperature indicates that this glass solution is
18 strongly supersaturated by sulindac at RT. This recrystallization persists until the
19 equilibrium saturated state is reached. Further heating then leads to the re-
20 dissolution of the previously recrystallized sulindac. This gives rise to the broad
21 endotherm that starts immediately after the end of the recrystallization and stops
22 around the melting temperature of pure sulindac.

23 Glass solutions PVP/sulindac could also be obtained by co-melting of physical
24 mixtures. This technique was used to determine the Gordon Taylor³⁶ plot of the

1 binary mixture which will be used in section 5 for the determination of solubility
2 curves. Physical mixtures PVP/sulindac of different compositions have been heated
3 (5°C/min) in the DSC just above the melting point of sulindac (200°C) and rapidly
4 cooled (20°C/min) down to 20°C. The quenched liquid mixture has then been
5 rescanned by heating at 5°C/min using the modulated temperature mode (modulation
6 amplitude: 0.663°C and modulation period: 50 sec). The reversible heat flow signals
7 recorded during the rescans are reported in figure 4 for sulindac weight fractions
8 ranging from 0 to 1. Each scan shows a single Cp jump which indicates that the co-
9 melting has produced a homogeneous glass solution. Moreover, the Tg of the glass
10 solution shifts toward the low temperatures for increasing sulindac concentration as a
11 results of its plasticizing effect. The evolution of Tg with the composition is reported in
12 figure 9 and appears to be almost linear. It has been fitted (figure 9 - solid line) by the
13 usual Gordon-Taylor law³⁶:

$$T_g(X_{sul}) = \frac{X_{sul} T_{g_{sul}} + K(1 - X_{sul}) T_{g_{PVP}}}{X_{sul} + K(1 - X_{sul})} \quad (1)$$

17
18 In this expression, $T_{g(sul)} = 75^\circ\text{C}$ and $T_{g(PVP)} = 110^\circ\text{C}$ are respectively the glass
19 transition temperatures of pure sulindac and pure PVP, X_{sul} is the sulindac fraction
20 and K is a fitting parameter characterizing the curvature of the evolution. The best fit
21 is obtained for $K = 0.85$. This value is very close to that expected for an ideal regular
22 solution^{36,37} which is given by equation (2):

23

1
$$K = \frac{\Delta C_{p(\text{PVP})}}{\Delta C_{p(\text{sul})}} = 0.87 \quad (2)$$

2 where $\Delta C_{p\text{PVP}} = 0.35 \text{ J/g/}^\circ\text{C}$ and $\Delta C_{p\text{sul}} = 0.40 \text{ J/g/}^\circ\text{C}$ are the amplitude of the Cp
3 jump at Tg determined respectively for pure PVP and pure sulindac. This suggests
4 that the interactions between the two chemical species, if any, are very weak.

5

6 **4.2 Formation of MCD by partial recrystallization of a glass solution under** 7 **plasticizing atmosphere**

8

9 The glass solution PVP/sulindac [15:85] previously obtained by co-milling has
10 been annealed for 3 hours at RT under an ethanol atmosphere (see section 2 for
11 details) and then dried at 100°C during 1h. It has been checked by TGA that after the
12 drying stage the sample does not contain any traces of ethanol. The X-ray diffraction
13 patterns recorded before and after the annealing and drying stages are reported in
14 figure 5. Before the annealing, the sample is clearly X-ray amorphous while it shows
15 many Bragg Peaks characteristic of form II after the annealing. This indicates that the
16 excess sulindac dispersed in the supersaturated glass solution has recrystallized
17 toward form II during the annealing. This recrystallization has been strongly facilitated
18 by the ethanol atmosphere which has increased the molecular mobility in the glass
19 solution through a plasticization effect. The average grain size of sulindac in the initial
20 PM and in the MCD has been estimated by polarized light microscopy. Figures 6a
21 and 6b compare crystalline sulindac in the PM and in the MCD. It appears that the
22 recrystallized grains of sulindac in the MCD are homogeneously dispersed inside the

1 amorphous polymer matrix and also much smaller than in the initial PM. Multiple
2 measurements of sulindac grain sizes indicate that the average grain size is close to
3 27 μm in the PM while it is close to close to 2 μm in the MCD. The smaller size of
4 sulindac grains in the MCD and their fine dispersion in the polymer matrix is thus
5 expected to strongly enhance the dissolution rate of crystalline sulindac.

6 Figure 7 compares the heating DSC scans (5°C/min) of the MCD to that of the
7 corresponding physical mixture. For the physical mixture (run 1), the thermogram
8 shows a Cp jump at 110°C corresponding to the glass transition of the PVP
9 component. It also shows, at higher temperature, a broad endotherm signaling the
10 dissolution of sulindac into PVP. Upon heating at 5°C/min, the onset of dissolution
11 starts around 135°C when the molecular mobility becomes high enough for the drug
12 molecule to diffuse into the polymer matrix on the time scale of the DSC scan. For
13 the MCD (run 2), both enthalpic events are also detected, but they are noticeably
14 shifted towards the low temperatures. The glass transition of the polymer matrix is
15 shifted by 13°C indicating that PVP is plasticized by a dispersed drug fraction
16 remaining in the matrix after the annealing. By reporting the glass transition
17 temperature (96°C) on the Gordon Talyor plot of the binary mixture (figure 9) it can
18 be estimated that the concentration of sulindac remaining molecularly dispersed into
19 the polymer is close to 34 %. This concentration thus corresponds to the solubility of
20 sulindac form II into the PVP matrix plasticized by ethanol at RT. At this stage, the
21 sample thus appears to be a MCD where 9 % of the drug is dispersed at the
22 molecular level and 91 % of the drug is dispersed in the form of tiny crystallites
23 whose average size is close to 2 μm (figure 6b). The dissolution endotherm is also
24 shifted toward the low temperature because of the higher molecular mobility arising

1 from the lower T_g. However, the shift of the onset of dissolution (26°C) is much larger
2 than the shift of the glass transition (13°C). This indicates that the molecular mobility
3 is not the only factor that facilitates the dissolution. The fine dispersion of the
4 crystallites inside the polymer matrix arising from the recrystallization of the glass
5 solution is also likely to be responsible for the easier dissolution of the drug. Because
6 of the fine dispersion, the interface drug-polymer is larger, the number of diffusion
7 center is bigger, and crystallites are embedded into the amorphous matrix. As a
8 result, drug molecules have to diffuse on smaller distances to increase
9 homogenously the concentration of drug molecules into the polymer matrix (figure 1).
10 It must also be noted that the dissolution endotherm ends at a lower temperature for
11 the MCD than for the PM. This means that the dissolution rate in the MCD is also
12 higher at high temperatures when dissolution reaches completion. MCD thus appears
13 to be a convenient system for all the methods that require to reach equilibrium
14 saturated states by dissolution of drug into the polymer. In section 5, MCD will be
15 used to determine the solubility curve of sulindac form II into PVP.

16 Interestingly, the glass solution obtained by co-milling recrystallizes toward
17 form I upon heating. This is clearly shown by the X-ray diffraction pattern (c) of figure
18 5 which has been recorded at RT after heating the sample at 140°C, i.e. in the
19 recrystallization range (figure 3 - run 3). However, this recrystallization is
20 accompanied by a decrease of the mobility in the polymer matrix due to a decrease
21 of the plasticization by the drug. As a result, the recrystallization becomes rapidly
22 strongly frustrated so that the recrystallized fraction is quite limited and does not
23 reach its equilibrium value. The recrystallization is also limited by the fact that the
24 solubility of sulindac in PVP increases with temperature. To get rid of these

1 limitations and to push further the recrystallization process, the sample partially
2 recrystallized at 140°C was annealed at RT under an ethanol atmosphere during 3
3 hours and then dried at 100°C under a dry atmosphere during 1 hour. The X-ray
4 diffraction pattern of the dried sample is reported in figure 5 (d). One can note a
5 noticeable development of Bragg peaks characteristic of form I which reveals a
6 deeper recrystallization toward this form. Moreover, the total absence of Bragg peaks
7 characteristic of form II indicates that the preexistence of form I has oriented the
8 recrystallization under ethanol atmosphere toward this form through a seeding effect.
9 The further crystallization of sulindac during the annealing under ethanol atmosphere
10 is also revealed by the glass transition which shifts of from 78°C to 94°C indicating
11 that the residual sulindac fraction has decreased from 0.85 to 0.39 The above
12 protocol thus provides MCD of form I into PVP that will be used in section 5 to
13 determine the solubility curve of sulindac form I into PVP.

14

15 **5. DETERMINATION OF PVP/SULINDAC SOLUBILITY CURVES**

16 In this section, we show how to take advantage of the faster dissolution rate of
17 crystallites embedded into the MCD to determine the solubility curve of sulindac
18 forms I and II into PVP.

19 The MCD was repeatedly scanned (5°C/min) by DSC. For each new scan, the final
20 temperature is increased by 10°C compared to the previous one and an annealing
21 was performed at the final temperature (T_a) to allow the MCD to reach equilibrium at
22 this temperature. The annealing time was set to 3 hours for annealing temperatures
23 ranging from 120°C to 160°C and reduced to 15 minutes above 160°C to avoid any

1 chemical degradation of the material at high temperatures. After each annealing, the
2 sample was rapidly cooled down to 20°C by removing the sample from the DSC and
3 placing it on a cold plate at -20°C. This fast cooling was used to avoid any
4 recrystallization of the fraction of sulindac previously dissolved at T_a in the polymer
5 matrix. Figure 8 shows the MDSC scans (reversible heat flow) recorded after
6 annealing performed at different temperatures T_a ranging from 120°C to 170°C. All
7 thermograms show a C_p jump corresponding to the glass transition of the molecular
8 dispersion component. This C_p jump shifts clearly toward the low temperatures and
9 its amplitude increases for increasing annealing temperatures. These effects are
10 clearly due to the dissolution of the drug that has occurred during the previous cycle
11 (heating and annealing at T_a). The supplementary dissolution increases both the
12 plasticization of the polymer and the fraction of amorphous dispersion.

13 The inset of figure 8 shows the heating MDSC scans (total heat flow) recorded after
14 the annealing at $T_a = 120^\circ\text{C}$ and $T_a = 130^\circ\text{C}$. They show an endothermic signal
15 corresponding to the dissolution that starts exactly at the temperature at which the
16 previous annealing has been performed. This proves that the equilibrium saturation
17 was effectively reached during this annealing. This behaviour was found to hold for
18 annealing between 120°C and 170°C as the dissolution rate increases with
19 temperature. On the other hand, it was found to fail below 120°C indicating that the
20 dissolution rate was too low to reach the equilibrium saturated state during the
21 annealing. It also fails above 170°C because the dissolution of sulindac is complete
22 after annealing at $T_a = 180^\circ\text{C}$. In that case, no more endothermic dissolution is
23 detected during the next scan.

24

1 Reporting the glass transition temperature measured after each annealing stage at T_a
2 (figure 8) on the Gordon Taylor curve (figure 9), then gives the equilibrium saturated
3 concentration corresponding to each annealing temperature T_a . The evolution of this
4 concentration with T_a is reported in figure 9. It corresponds to the solubility curve of
5 sulindac form II into PVP. It must be noted that equilibrium saturation states cannot
6 be obtained above 170°C as the corresponding drug concentration is higher than the
7 effective drug concentration in the sample. It cannot be obtained either below 120°C
8 as the dissolution rate is too low to reach the saturation within the three hour
9 annealing stage.

10 The same protocol has been implemented for MCD of form I into PVP to determine
11 the solubility line of form I into PVP between 120°C et 180°C. The results are
12 reported in figure 9. Interestingly, the solubility curves of forms I and II cross around
13 150°C. Such a behavior is coherent with the fact that forms I and II were recently
14 shown to form an enantiotropic system with a polymorphic transition expected around
15 160°C^{35,38}. This is also coherent with the fact that metastable forms are expected to
16 be more soluble than stable ones.

17

1 5. CONCLUSION

2

3 In this paper we have presented an original and efficient method to determine
4 the solubility curve of drugs into polymers. The idea is to use molecular/crystalline
5 dispersions (MCD) for which the drug is dispersed in the polymer, partly at the
6 molecular level and partly in the form of small crystals. This particular microstructure
7 greatly increases the rate of dissolution of the crystalline fraction because: (1) drug
8 molecules already dispersed in the polymer have a plasticizing effect which greatly
9 increases the molecular mobility in the amorphous matrix. (2) The fine dispersion of
10 the small crystals in the amorphous matrix strongly reduces the distances over which
11 the drug molecules belonging to the crystallites must diffuse to invade
12 homogeneously the amorphous matrix by dissolution.

13 MCD were here obtained in two steps: First, a strongly supersaturated glass
14 solution is obtained by forcing the co-amorphisation the two compounds directly in
15 the solid state by high energy mechanical milling². Second, a strong recrystallization
16 of the glass solution is made possible by annealing the glass solution at RT under a
17 plasticizing atmosphere. After drying, this two-step protocol provides a molecular and
18 crystalline dispersion (MCD) for which the drug is dispersed in the polymer, partly at
19 the molecular level and partly in the form of small crystals. It must be noted that the
20 recrystallization of the glass solution occurs naturally, using the easiest pathway and
21 with the lowest energy cost. The resulting dispersion (size and repartition of
22 crystallites) is thus expected to be that which best facilitates the inverse process of
23 (re)dissolution of the crystallites. Moreover, the nature of the polymorph that

1 recrystallizes to form the MCD can be controlled by seeding or by changing the
2 plasticizing atmosphere. MCDs of sulindac form I and II into PVP could thus be
3 selectively obtained.

4 We have taken advantage of the higher dissolution rates of these MCDs to
5 determine the solubility lines of the polymorphic forms I and II of sulindac into PVP.
6 Equilibrium saturated states were reached at different temperatures by annealing
7 MCDs at these temperatures. The fraction of drug dissolved in PVP was then derived
8 directly from the T_g of the saturated state, using the Gorton Taylor curve of the
9 mixture as a calibration curve.

10 The method presented in this paper has three main advantages: (i) The
11 equilibrium saturated states can be obtained in a reasonable time. (ii) The whole
12 solubility curve can be obtained in the course of a single DSC experiment using only
13 one sample. (iii) It gives access to the solubility curve of several polymorphs of a
14 given drug.

15

16

17 **ACKNOWLEDGEMENTS**

18 This project has received funding from the Interreg 2 Seas programme 2014-2020
19 co-funded by the European Regional Development Fund under subsidy contract
20 2S01-059_IMODE

21

Captions

Figure 1 Schematic pointing out the advantage of MCD over PM to reach faster the equilibrium saturated state of a drug/polymer mixture. The bottom part shows how to convert PM into MCD using milling and annealing under a plasticizing atmosphere. Green lines symbolize the polymer. Red dots and red blocs symbolize respectively molecules and crystallites of drug.

Figure 2 Powder X-ray diffraction patterns recorded at room temperature:

- (a) crystalline sulindac: non milled
- (b) crystalline sulindac: milled (10h)
- (c) PVP K12: non milled
- (d) PVP K12: milled (10 h)
- (e) physical mixture of sulindac and PVP [85:15]_{w/w}: non milled
- (f) physical mixture of sulindac and PVP [85:15]_{w/w}: co-milled (10h)

Figure 3 DSC scans recorded upon heating (5°C/min):

- run 1: crystalline sulindac: non milled
- run 2: crystalline sulindac: milled (10h)
- run 3: physical mixture of sulindac and PVP [85:15]_{w/w}: co-milled (10h)
- run 4: PVP K12: non milled
- run 5: PVP K12: milled (10h)

Figure 4 MDSC scans (reversible heat flow) of PVP/sulindac glass solutions recorded upon heating. The fraction of sulindac (X_{sul}) varies from 0 to 1. Glass solutions were obtained by co-melting the corresponding physical mixtures at 200°C and by quenching the melt at 20°C. Scans were recorded at 5°C/min using a modulation amplitude of 0.663°C and a modulation period of 50 sec.

Figure 5 Powder X-ray diffraction patterns (recorded at RT) of a physical mixture PVP/sulindac [85:15]_{w/w} co-milled during 10h:

- (a) Just after co-milling
- (b) After annealing for 3h under ethanol atmosphere and drying for 1h at 100°C under dry atmosphere.
- (c) After recrystallization at 140°C.
- (d) After recrystallization at 140°C, annealing for 3h at RT under ethanol atmosphere, and drying for 1h at 100°C under dry atmosphere.

PXRD patterns of crystalline forms I and II are also reported for comparison.

Figure 6 Pictures obtained by Cross-polarized light microscopy:
a) Commercial crystalline grains of sulindac(form II) used for physical mixtures (PM)
b) MCD (II) obtained by annealing a glass solution PVP/sulindac [85:15]_{w/w} for 3h at RT under an ethanol atmosphere (see section 2 for details) and then drying at 100°C during 1 h.

Figure 7 Heating DSC scans (5°C/min) of sulindac/PVP [85:15]_{w/w} mixtures.
run 1: Physical mixture (PM)
run 2: Molecular / crystalline dispersion (MCD) obtained by co-milling the PM for 10h, annealing for 3h at RT under ethanol atmosphere (see section 2 for details) and drying at 100°C during 1h

Figure 8 MDSC scans (reversible heat flow) of MCD PVP / sulindac [15:85]_{w/w} recorded after annealing the sample at different temperatures ranging between 120°C and 170°C as indicated on the right hand part of the figure. Scans were recorded at 5°C/min using a modulation amplitude of 0.663°C and a modulation period of 50 sec.
The inset shows the total heat flow signal recorded upon heating (5°C/min) after the annealing at 120°C and 130°C. It shows that the onset of dissolution upon heating occurs exactly at the temperature at which the annealing was performed.

Figure 9 In black: Gordon Taylor plot ($T_g(X_{sul})$) of sulindac/PVP glass solution. The full circles correspond to experimental T_g values derived from the DSC scans of figure 4. The solid line represents the best fit of equation 1 on the data.
In red and in green: Solubility curve of form I and form II of sulindac into PVP as a function of temperature. The full circles correspond to experimental data. Solid lines are guides for eyes.

Figure 1

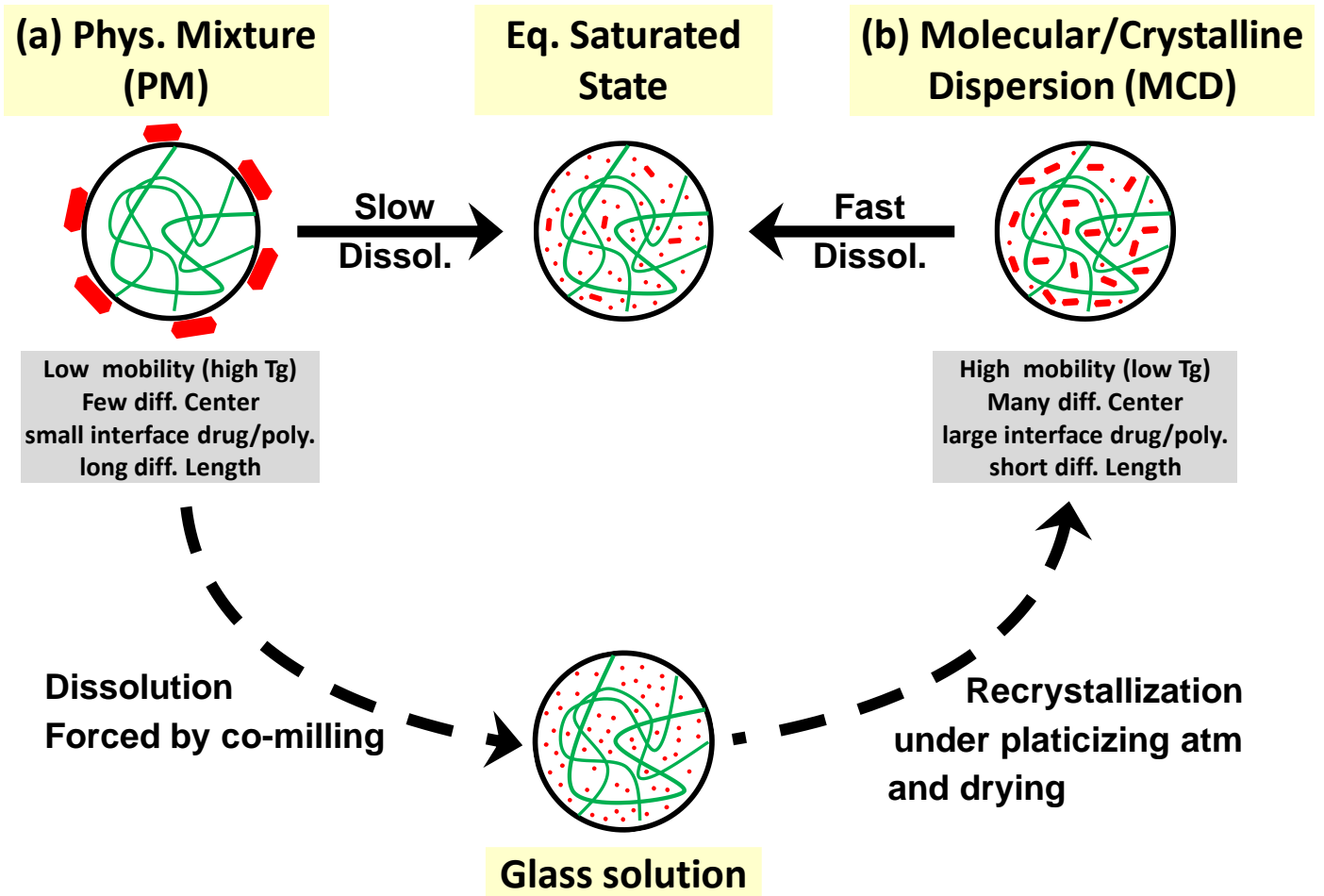


Figure 2

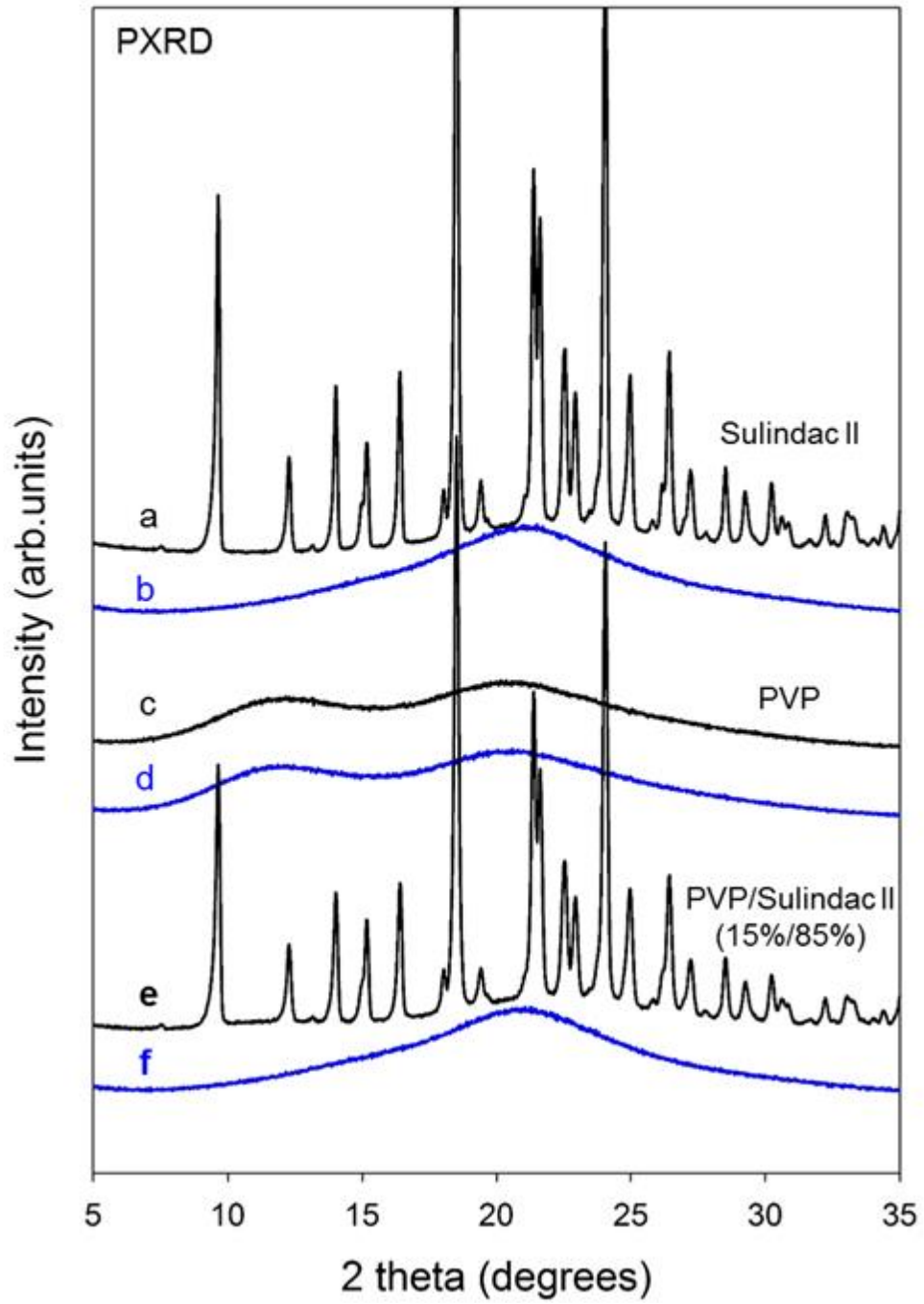


Figure 3

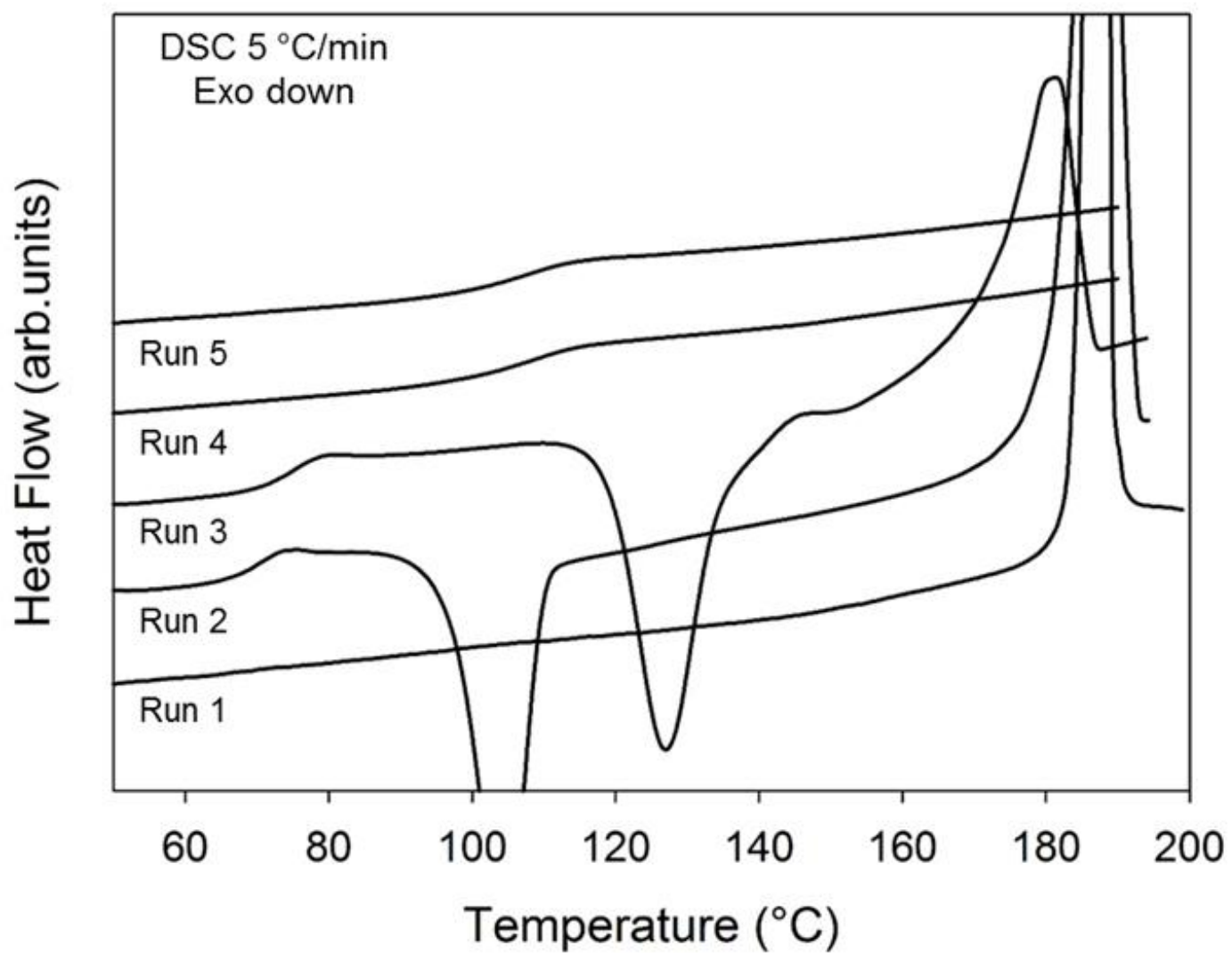


Figure 4

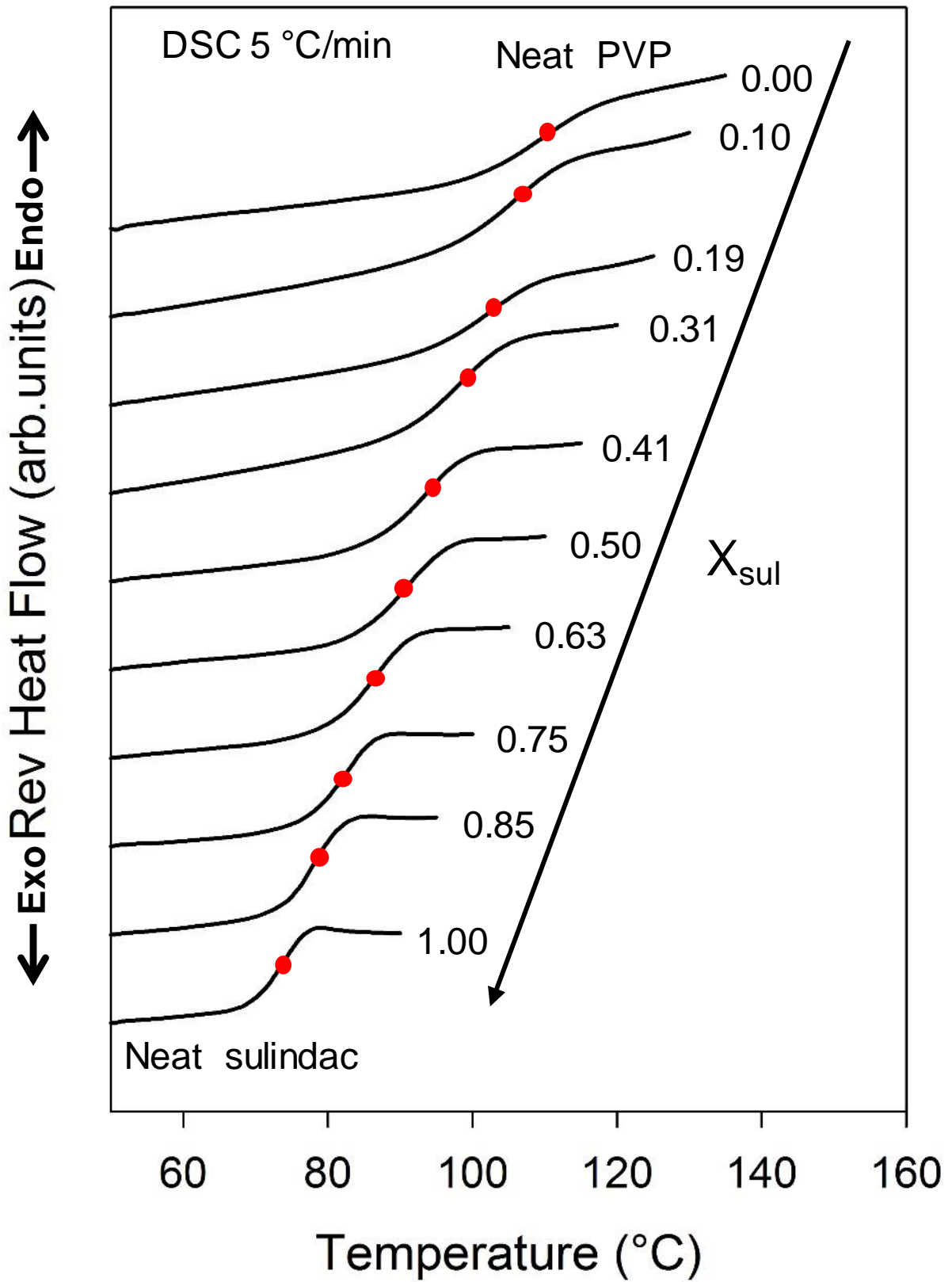


Figure 5

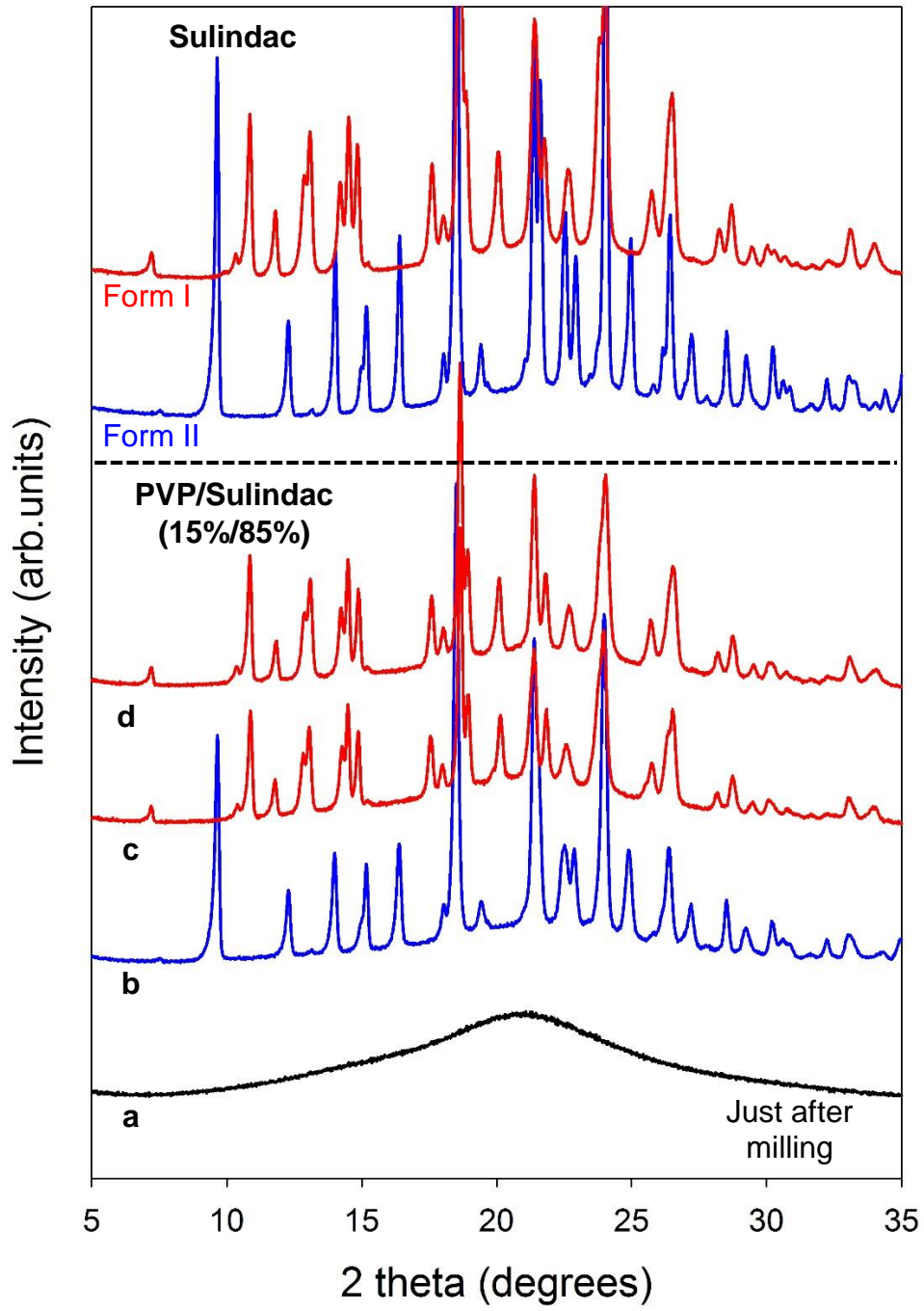


Figure 6

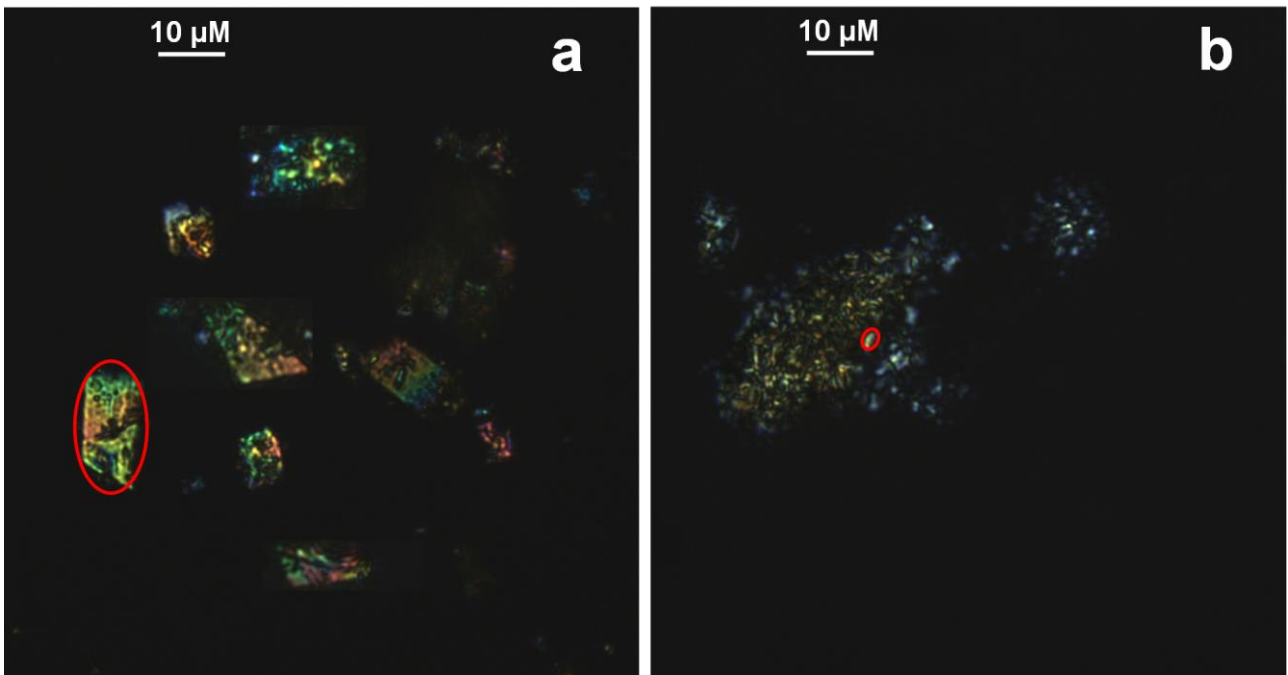


Figure 7

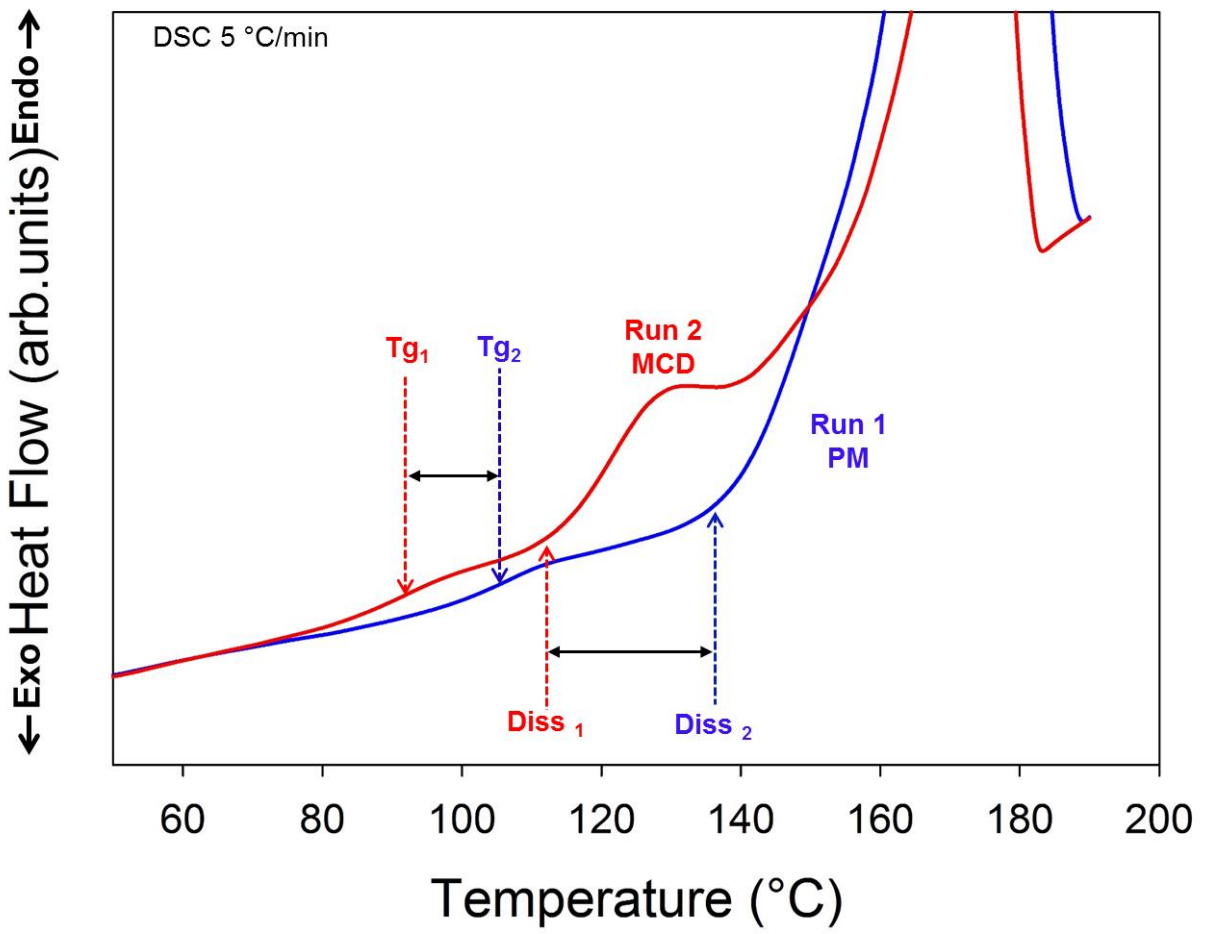


Figure 8

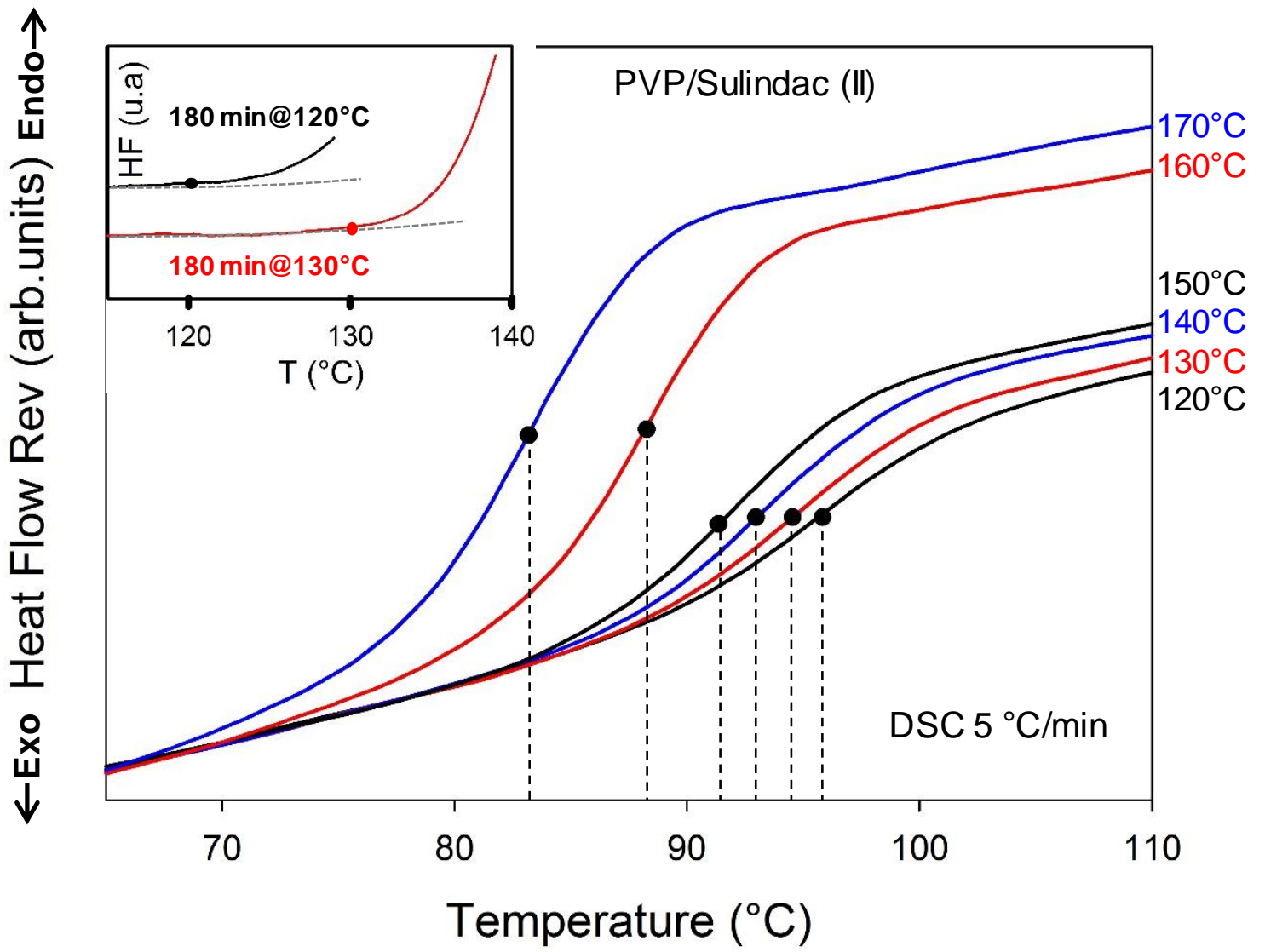
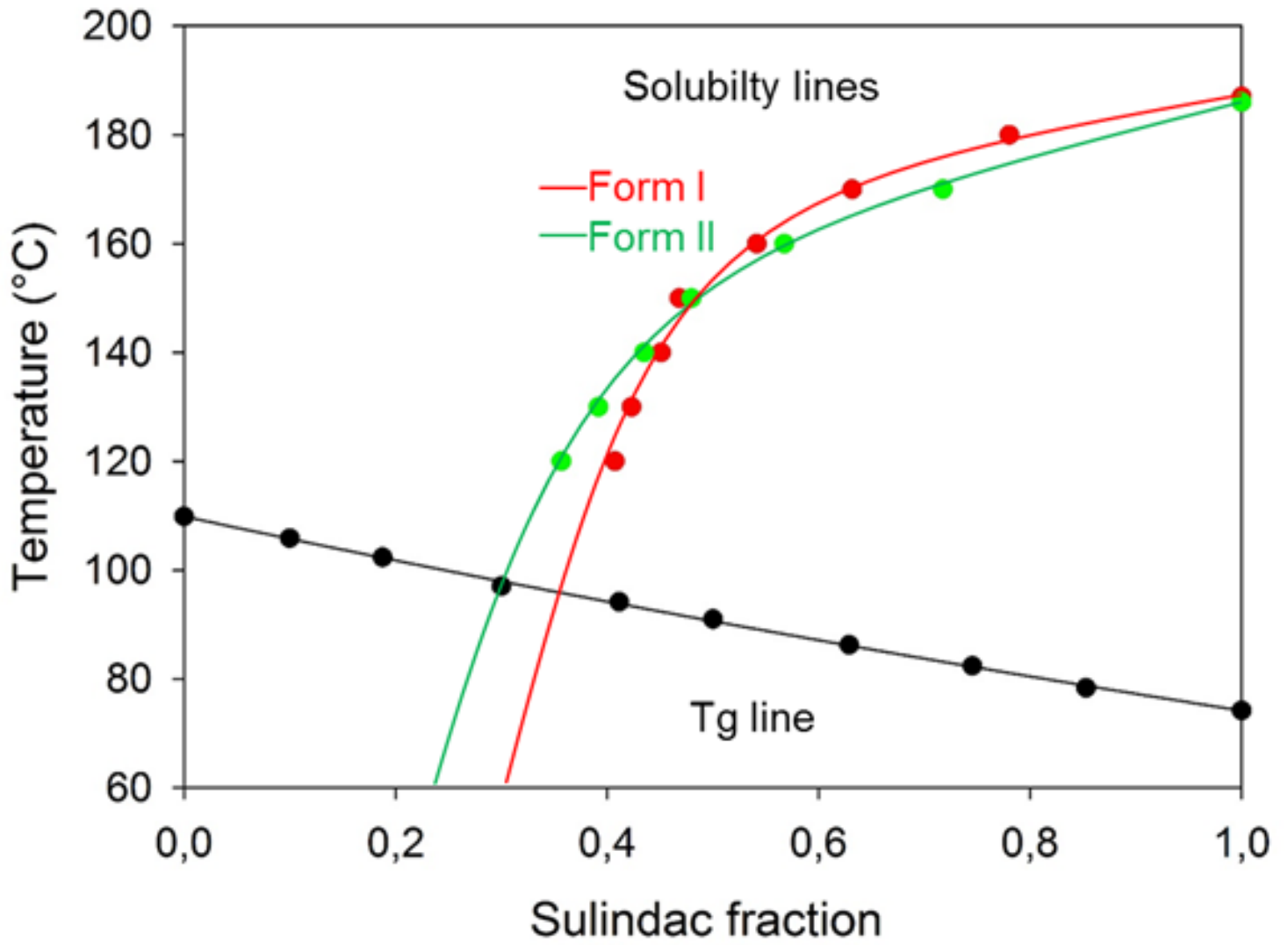


Figure 9



References

1. Johari GP, Shanker RM 2014. On the solubility advantage of a pharmaceutical's glassy state over the crystal state, and of its crystal polymorphs. *Thermochimica Acta* 598:16-27.
2. Babu NJ, Nangia A 2011. Solubility Advantage of Amorphous Drugs and Pharmaceutical Cocrystals. *Crystal Growth & Design* 11(7):2662-2679.
3. Blagden N, de Matas M, Gavan PT, York P 2007. Crystal engineering of active pharmaceutical ingredients to improve solubility and dissolution rates. *Advanced Drug Delivery Reviews* 59(7):617-630.
4. Sun Y, Zhu L, Wu T, Cai T, Gunn EM, Yu L 2012. Stability of Amorphous Pharmaceutical Solids: Crystal Growth Mechanisms and Effect of Polymer Additives. *The AAPS Journal* 14(3):380-388.
5. Yu L 2016. Surface mobility of molecular glasses and its importance in physical stability. *Advanced Drug Delivery Reviews* 100:3-9.
6. Bhattacharya S, Suryanarayanan R 2009. Local mobility in amorphous pharmaceuticals-characterization and implications on stability. *Journal of Pharmaceutical Sciences* 98(9):2935-2953.
7. Gupta P, Chawla G, Bansal AK 2004. Physical stability and solubility advantage from amorphous celecoxib: the role of thermodynamic quantities and molecular mobility. *Mol Pharm* 1(6):406-413.
8. Graeser KA, Patterson JE, Rades T 2008. Physical stability of amorphous drugs: Evaluation of thermodynamic and kinetic parameters. *Journal of Pharmacy and Pharmacology* 60:116.
9. Hancock BC, Parks M 2000. What is the true solubility advantage for amorphous pharmaceuticals? *Pharmaceutical Research* 17(4):397-404.
10. Murdande SB, Pikal MJ, Shanker RM, Bogner RH 2010. Solubility advantage of amorphous pharmaceuticals: I. A thermodynamic analysis. *Journal of Pharmaceutical Sciences* 99(3):1254-1264.
11. Vasconcelos T, Sarmento B, Costa P 2007. Solid dispersions as strategy to improve oral bioavailability of poor water soluble drugs. *Drug Discovery Today* 12(23-24):1068-1075.
12. Patel RC, Masnoon S, Patel MM, Patel NM 2009. Formulation strategies for improving drug solubility using solid dispersions. *Pharmaceutical Reviews* 7(6).
13. Bhugra C, Telang C, Schwabe R, Zhong L 2016. Reduced crystallization temperature methodology for polymer selection in amorphous solid dispersions: Stability perspective. *Molecular Pharmaceutics* 13(9):3326-3333.
14. Newman A, Knipp G, Zografis G 2012. Assessing the performance of amorphous solid dispersions. *Journal of Pharmaceutical Sciences* 101(4):1355-1377.
15. Jaskirat S, Manpreet W, Harikumar SL 2013. Solubility enhancement by solid dispersion method: a review. *Journal of Drug Delivery & Therapeutics* 3(5):148-155.
16. Leuner C, Dressman J 2000. Improving drug solubility for oral delivery using solid dispersions. *European Journal of Pharmaceutics and Biopharmaceutics* 50(1):47-60.
17. Laitinen R, Priemel PA, Surwase S, Graeser K, Strachan CJ, Grohgan H, Rades T. 2014. Theoretical Considerations in Developing Amorphous Solid Dispersions. In Shah N, Sandhu H, Choi DS, Chokshi H, Malick AW, editors. *Amorphous Solid Dispersions*, ed.: Springer New York. p 35-90.
18. Padden BE, Miller JM, Robbins T, Zocharski PD, Prasad L, Spence JK, LaFountaine J 2011. Amorphous solid dispersions as enabling formulations for discovery and early development. *American Pharmaceutical Review* 14(1):66-73.
19. Knopp MM, Gannon N, Porsch I, Rask MB, Olesen NE, Langguth P, Holm R, Rades T 2016. A Promising New Method to Estimate Drug-Polymer Solubility at Room Temperature. *Journal of Pharmaceutical Sciences* 105(9):2621-2624.
20. Mahieu A, Willart J-F, Dudognon E, Danède F, Descamps M 2013. A New Protocol To Determine the Solubility of Drugs into Polymer Matrixes. *Molecular Pharmaceutics* 10(2):560-566.

21. Marsac PJ, Li T, Taylor LS 2009. Estimation of drug-polymer miscibility and solubility in amorphous solid dispersions using experimentally determined interaction parameters. *Pharmaceutical Research* 26(1):139-151.
22. Marsac PJ, Shamblin SL, Taylor LS 2006. Theoretical and practical approaches for prediction of drug-polymer miscibility and solubility. *Pharmaceutical Research* 23(10):2417-2426.
23. Llinas A, Box KJ, Burley JC, Glen RC, Goodman JM 2007. A new method for the reproducible generation of polymorphs: two forms of sulindac with very different solubilities. *Journal of Applied Crystallography* 40(2):379-381.
24. Chung Hoe Koo, Sang Hern Kim, Wanchui Shin 1985. Crystal Structure of Antiinflammatory Sulindac. *Bulletin of the Korean Chemical Society* 6(4):222-224.
25. Grzesiak AL, Matzger AJ 2007. New Form Discovery for the Analgesics Flurbiprofen and Sulindac Facilitated by Polymer-Induced Heteronucleation. *Journal of pharmaceutical sciences* 96(11):2978-2986.
26. Tao J, Sun Y, Zhang GGZ, Yu L 2008. Solubility of Small-Molecule Crystals in Polymers: d-Mannitol in PVP, Indomethacin in PVP/VA, and Nifedipine in PVP/VA. *Pharmaceutical Research* 26(4):855-864.
27. Sun Y, Tao J, Zhang GGZ, Yu L 2010. Solubilities of crystalline drugs in polymers: An improved analytical method and comparison of solubilities of indomethacin and nifedipine in PVP, PVP/VA, and PVAc. *Journal of Pharmaceutical Sciences*:n/a-n/a.
28. Bellantone RA, Patel P, Sandhu H, Choi DS, Singhal D, Chokshi H, Malick AW, Shah N 2012. A method to predict the equilibrium solubility of drugs in solid polymers near room temperature using thermal analysis. *Journal of Pharmaceutical Sciences* 101(12):4549-4558.
29. Amharar Y, Curtin V, Gallagher KH, Healy AM 2014. Solubility of crystalline organic compounds in high and low molecular weight amorphous matrices above and below the glass transition by zero enthalpy extrapolation. *International-journal-of-pharmaceutics* 472(1-2):241-247.
30. Willart JF, Descamps M 2008. Solid State Amorphization of Pharmaceuticals. *Molecular Pharmaceutics* 5(6):905-920.
31. Willart JF, Dudognon E, Descamps N, Larsson T, Descamps M 2006. Lactose-based molecular alloys obtained by solid state vitrification. *Journal of Non-Crystalline Solids* 352(42-49):4475-4479.
32. Nagahama M, Suga H 2002. Molecular alloys formed by solid-state vitrification. *Journal of Molecular Liquids* 95(3):261-284.
33. Nagahama M, Suga H, Andersson O 2000. Formation of molecular alloys by solid-state vitrification. *Thermochimica Acta* 363(1-2):165-174.
34. Guerra RB, Gálico DA, Holanda BBC 2016. A new method for the reproducible generation of polymorphs: two forms of sulindac with very different solubilities. *J Therm Anal Calorim* 123:2523-2530.
35. Latreche M, Willart JF, Guerin M, Hédoux A, Danède F 2019. Using Milling to Explore Physical States: The Amorphous and Polymorphic Forms of Sulindac. *Journal of Pharmaceutical Sciences*.
36. Gordon JM, Rouse GB, Gibbs JH, Risen WM, Jr. 1977. The composition dependence of glass transition properties. *Journal of Chemical Physics* 66(11):4971-4976.
37. Couchman PR, Karasz FE 1978. A Classical Thermodynamic Discussion of the Effect of Composition on Glass-Transition Temperatures. *Macromolecules* 11(1):117-119.
38. Tung HH, Paul EL, Midler M, McCauley JA. 2009. *Crystallization of Organic Compounds: An Industrial Perspective*. ed.: Wiley.